

TRANSIENT FEEDBACK FROM FUEL MOTION IN METAL IFR FUEL

Report No. 1
MAY 04 1990

E. A. Rhodes, G. S. Stanford, J. P. Regis,
T. H. Bauer, and C. E. Dickerman

CONF-900804--5

Argonne National Laboratory
Argonne, Illinois 60439, U.S.A.

DE90 010136

ABSTRACT

Results from hodoscope data analyses are presented for TREAT transient-overpower tests M5 through M7 with emphasis on transient feedback mechanisms, including prefailure expansion at the tops of the fuel pins, subsequent dispersive axial fuel motion, and losses in relative worth of the fuel pins during the tests. Tests M5 and M6 were the first TOP tests of margin to cladding breach and prefailure elongation of D9-clad ternary (U-Pu-Zr) IFR-type fuel. Test M7 extended these results to high-burnup fuel and also initiated transient testing of HT9-clad binary (U-Zr) FFTF-driver fuel. Results show significant prefailure negative reactivity feedback and strongly negative feedback from fuel driven to failure.

INTRODUCTION

One key aim of the M-series transient overpower simulations performed at the Transient Reactor (TREAT) facility is measurement of axial fuel expansion as a reactivity-reduction mechanism to prevent fuel failure. Transient fuel-motion data have been analyzed from experiments on Integral Fast Reactor (IFR) reference ternary-alloy fuel (tests M5F1, M5F2, M6, and M7).¹ These experiments span a range of burnup of 0.8 to 9.9 a/o. Results show the favorable characteristics of prefailure fuel expansion, high margin to transient failure, and highly dispersive post-failure fuel motion found in initial TREAT experiments with irradiated metallic U-²³⁵ Experimental Breeder Reactor II (EBR-II) fuel.²

Fuel-motion data were obtained using the TREAT fast-neutron hodoscope.³ This instrument contains an array of detectors behind slots in a collimator that project onto a 10-column by 36-row rectangular grid of 62 mm total width and 1215 mm total height at the test section centerline (51 mm north of the reactor centerline). By collecting counts from fission neutrons at down to millisecond intervals, the time evolution of a two-dimensional image of the test-fuel fission density is obtained.

In each experiment, two test-pin fuel columns, each nominally 343 mm long and 4.3 mm in diameter, were held side-by-side in two separate flow tubes that were far enough apart for the hodoscope to resolve the fuel motion in each pin. The test pins were contained in a Mark-III TREAT Integral Sodium Loop. Sodium flow, initial temperature, and the reactor power-vs-time profile were set to generate prototypic thermal conditions in each test pin. Each of the experiments simulated a postulated transient overpower accident with 8-second exponential period, continued until the region of incipient or actual cladding failure was reached. This

caused peak test-fuel temperature rise rates of about 100 K/s (at the high end of the range of heating rates relevant to potential IFR accidents). Table I below summarizes the changes in length and relative worth during the tests for each pin, in order of increasing burnup, as determined from hodoscope data.

TABLE I
Hodoscope Fuel-Motion Data for TREAT Tests M5 - M7

Pin ^a	Burnup, a/o	Length Increase, %	Relative Worth Change, %		
			Prefailure	Post-failure	Total
M5F1W ^b	0.8	0.8	-1.0	N.A.	-1.0
M5F2W ^b	0.8	0.4	-1.0	N.A.	-1.0
M5F1E ^b	1.9	0.0	-0.8	N.A.	-0.8
M5F2E ^b	1.9	2.5	-2.3	N.A.	-2.3
M6W	1.9	3.0	-5.0	N.A.	-5.0
M7E ^c	2.9	3.7	-1.9	N.A.	-1.9
M6E	5.3	N.A. ^d	-6.2	-16.8	-23.0
M7W	9.8	N.A. ^d	-4.5	-21.0	-25.5

^aW denotes West pin; E, East pin; preceding letters, TREAT test.

^bBoth M5F1 pins were run again in M5F2. The length and worth changes listed for M5F2 are in addition to those measured for M5F1.

^cPin M7E is HT9-clad U-Zr; all other pins are D9-clad U-Pu-Zr.

^dTest pin was driven to failure.

Fuel length changes listed in Table I were obtained by scanning the hodoscope collimator vertically over the test section at low reactor power before and after the experiment, and comparing the resulting mass distributions. Transient mass distributions were obtained from the hodoscope transient data. Since these measurements yield quantitative fuel-mass distributions inside and outside the active fuel columns, rather than just overall fuel length, they can be used to describe reactivity feedback, which depends upon the change in overall spatial fuel distribution.

In order to provide a global datum to describe the significance of fuel redistributions in each experiment, the axial distribution of fuel at a given time is multiplied by a cosine-squared axial worth distribution appropriate to EBR-II and integrated axially. Changes in this quantity then provide an approximate reactivity-feedback worth value indicating the significance of the fuel distribution changes, assuming all of the fuel in the fast reactor were to coherently undergo the mass redistribution of the test pin. Two relative changes in worth are given in the table: the maximum prefailure value and (where applicable) the post-failure value. Data indicate that both pins that were driven to failure failed in the top region of the fuel.

DATA NORMALIZATIONS AND REPRESENTATIONS

The general aspects of hodoscope data normalizations and representations are discussed comprehensively in Ref. 3. Here a brief discussion of the most basic considerations is presented specific to the M-series tests. The largest uncorrected effect in these tests is power coupling changes in the test fuel, caused by control-rod motion during and after shutdown and by test-fuel self-shielding changes due to fuel expansion and dispersive fuel motion (in the case of cladding failure). The largest self-shielding changes occur after a pin failure, when the dispersing fuel moves from a highly-shielded location inside the pin to a nearly unshielded location above the pin. This effect is compensated to some degree by normalization methods used but it still causes worth losses to be underestimated, leading to a conservative estimate of negative reactivity feedback.

In order to have uniform response to test-fuel mass, each channel count rate was corrected for detector efficiency and compensated for reactor flux variation over the view field. Count rates must also be divided by a quantity proportional to the fast neutron flux, to remove transient variation of reactor power as a source of count rate change. In the case of integral hodographs (Figs. 1 and 2), each count rate was divided by the count rate average over the entire view field, which conserves test-fuel mass over the view field. However small systematic inaccuracies will be present due to self-shielding changes and will increase in effect as fuel leaves the view field (in the case of pin failure). For worth time evolution (Figs. 3-6), count rates for each pin were divided separately by the average over channels viewing only each pin, to further limit the effect of power-coupling variations.

Displayed in Figs. 1 and 2 are a selection of integral hodographs depicting fuel motion evolution in the M6 and M7 experiments as a sequence of two-dimensional fuel-mass projections, averaged over the transient times shown. A test-fuel mass scale was derived by multiplying channel count rates by a mass calibration factor determined from the total known test-fuel mass, after subtracting a uniform background. The mass viewed by a specific channel is indicated by a black symbol whose size increases with mass. For example, the smallest symbol on the scale shown represents 0.25 to 0.75 g (midpoint 0.5 g). Response to the east pin fuel columns occurs mainly in hodoscope column 6 and response to the west pin fuel columns is mainly shared by hodoscope columns 3 and 4. The hodographs are greatly expanded in the horizontal dimension compared to the vertical, as the interchannel spacing is 6.18 mm horizontally and 33.76 mm vertically.

Shown in Figs. 3-6 are the relative worth vs. elapsed transient time plots for the individual pin fuel columns in each of the experiments. Worth is computed as $\sum_i w_i (R_i - B)$, where w_i is the worth weight for hodoscope row i , R_i is the normalized count rate for row i (averaged over hodoscope columns viewing the pin), and B is background. Relative worth in the figures is divided by the average of the first 15 time segments shown in each plot. The worth weight used is a cosine-squared function centered on the fuel column, scaled to a FWHM of 0.81 times the length of the fuel column, and truncated at the first node above and below the fuel column. This function provides quantitative continuity in transient analysis. It presents a reasonable generic shape, has been used in analysis of past transients,⁴ and yields worth time evolutions very similar to those obtained for these tests using computed SAFR and PRISM worth weights scaled to length and positioned properly on the fuel pins.

The worth changes shown in Figs. 3-6 corresponding to sudden and/or rapid expansion and to clad failure are somewhat smaller than the prefailure and post-failure worth changes given in Table I. This is because the worth changes corresponding to rapid expansion do not include earlier small worth losses from thermal expansion of the fuel, and because the worth change percentages in the plots corresponding to clad failure are calculated against the immediately preceding relative worth (which is less than 1). For the M7 9.8% burnup pin, estimates were made of corrections to worth changes, mainly for self-shielding changes. Note that the corrected worth loss due to clad failure is estimated to nearly double in value to $\sim -40\%$.

TRANSIENT AXIAL FUEL-MOTION ANALYSIS

The power profile for test M5F1 indicates power decrease due to shutdown occurred at ~ 15.6 s. The west fuel column (0.8% burnup) underwent a small elongation that accelerated somewhat at ~ 11.5 s and reached a maximum of $\sim 0.9\%$ at shutdown, corresponding to a 1.04% worth loss (Fig. 3), after which it decreased to 0.8% (Table I). The east fuel column (1.9% burnup) underwent a small transient elongation that accelerated at ~ 12.0 s and also reached a maximum at shutdown, $\sim 0.5\%$ along with a worth loss of 0.82%, and afterwards apparently contracted back to near its original length (Table I).

Since the same test-train configuration was used for both M5F1 and M5F2, the two fuel columns are the same. The power decrease due to shutdown began at ~ 16.2 s for M5F2. The west fuel column (0.8% burnup) had a small elongation that accelerated at ~ 12.0 s and reached $\sim 0.7\%$ maximum at shutdown, corresponding to a 0.96% worth loss (Fig. 4), after which it decreased to 0.4% (Table I). The east fuel column (1.9% burnup) underwent a more significant elongation that began accelerating at ~ 11.5 s and became more sudden at ~ 15.7 s, measuring $\sim 1.7\%$ at shutdown, corresponding to 2.27% worth decrease. Table I records a 2.5% post-test elongation.

The axial fuel-motion events occurring in the M6 transient can be keyed to the hodograph sequence in Fig. 1 and the worth curves in Fig. 5. The west (1.9% burnup) pin exhibited an expansion that may have been more of a local swelling than an elongation or extrusion. The start of rapid expansion began with a 20-40 ms event at 11.60 ± 0.03 s that involved a small jump in count rate in row 13 followed quickly by a small jump in row 12 count rate; an associated 1.56% worth decrease is seen in Fig. 5. The count rate in row 12 then remained constant, but the increase continued in row 13 until 13.1 ± 0.1 s, and a gradual decrease began after shutdown started at 13.255 ± 0.005 s. The total worth decrease at shutdown is 5.0% (Table I). If the event is regarded as an elongation, a maximum value of 2.9% is obtained (consistent with the 3.0% value from the post-test scan).

Figure 1b shows the expansion of both M6 fuel columns against the reference interval in Fig. 1a. The east (5.3% burnup) pin underwent rapid expansion beginning at 11.75 ± 0.05 s and fuel ejection (from cladding failure) was observed beginning at 13.235 ± 0.005 s, seen in Fig. 1c. The front of fuel ejected upward can be seen in Figs. 1d-1f along with depletion of fuel in the original column. Fuel apparently went above the hodoscope view field, and fuel motion appeared to have stopped by ~ 13.5 s. Maximum elongation was computed to be 2.9% just prior to failure. From Fig. 5, a 3.6% worth decrease comes from rapid

elongation, an 18.0% decrease from cladding failure, a total 23.0% worth decrease (Table I). The appearance of ejected fuel in hodoscope column 5, to the side of the east pin, provided the opportunity to more directly observe cladding failure location and velocities of ejected fuel. Failure location was determined to be at the top of the fuel column, with initial axial ejection velocities \sim 4.2 m/s upward and \sim 2.8 m/s downward.

The M7 hodograph sequence is shown in Fig. 2, with worth curves in Fig. 6. Figure 2b shows the expansion of both M7 fuel columns against the reference interval in Fig. 2a. The west (9.8% burnup) pin initially underwent a slow upward expansion of \sim 0.2% that became more rapid beginning at \sim 15.0 s and terminated in fuel expulsion above the fuel column (due to cladding failure) beginning at 17.711 ± 0.0025 s, as shown in Figs. 2c, and 2d. Just before cladding failure, the maximum elongation was \sim 2.9%, with a worth decrease of \sim 4.5% (from Table I). As shown in Figs. 2e-2f, fuel expulsion continued upward to above the view field, being slowed by shutdown beginning at 17.755 ± 0.008 s, motion being completed by \sim 20 s. The worth decrease associated with cladding failure was \sim 21.6% (Fig. 6) and the total worth decrease was \sim 25.5% (Table I). Fuel was ejected upward in perhaps several spurts, with an initial front velocity of \sim 11 to 13.5 m/s, and a substantial amount of fuel left the fuel column.

Unlike the other test pins in the series of experiments reported here, the M7 east pin contains binary (U-Zr) rather than ternary (U-Pu-Zr) alloy fuel, sheathed in HT-9 rather than D-9 cladding. This fuel column underwent a slow upward expansion to \sim 0.3%, followed by a very sudden upward expansion starting at 17.328 ± 0.002 s, with most of the expansion occurring over \sim 5 ms (see Figs. 2a-2c). No further axial fuel motion appeared to take place after this sudden expansion. A worth decrease of \sim 1.85% is associated with the sudden expansion (Fig. 6). The expansion may have been more like local swelling than elongation, but if it is presumed to be elongation, a value of \sim 1.8% is found (however a value of \sim 3.7% is found from the post-test scan). A clue to the type of fuel displacement comes from the post-test radiographs, which show a complete separation of the fuel column extending from \sim 32 mm to \sim 38 mm from the top of the fuel-column.

SUMMARY OF FUEL-MOTION ANALYSIS

Hodoscope data and post-test radiographic data are basically consistent with the fuel motion reported. All pins in the full 0.8 to 9.9 a/o burnup range tested exhibit high margins to transient failure, with significant worth loss from prefailure fuel expansion. In the pins driven to failure, clad breach occurred at the most favorable location, the top of the fuel column, with substantial subsequent worth loss from the highly dispersive post-failure fuel motion.

These favorable characteristics are similar to those found in initial TREAT experiments with irradiated metallic U-fs EBR-II fuel,² except that the prefailure fuel expansion for the fuel pins investigated herein is smaller at low burnup and does not exhibit a strong dependence on burnup. Depending on the amount of fuel-motion coherence among fuel pins involved in an actual transient overpower condition, the reactivity feedback mechanisms investigated might be sufficient to either prevent failure or to terminate the accident following failure.

ACKNOWLEDGMENT

This work was supported by the U. S. Department of Energy, Technology Support Programs, under contract W-31-108-Eng-38.

REFERENCES

1. T. H. BAUER, A. E. WRIGHT, W. R. ROBINSON, J. W. HOLLAND, and E. A. RHODES, "Behavior of Modern Metallic Fuel in TREAT Transient Overpower Tests", submitted to Nucl. Tech.
2. T. H. BAUER, A. E. KLICKMAN, R. K. LO, E. A. RHODES, W. R. ROBINSON, G. STANFORD, and A. E. WRIGHT, "Behavior of Metallic Uranium-Fissium Fuel in TREAT Transient Overpower Tests", Trans. Amer. Nucl. Soc. **53**, 306 (1986).
3. A. DEVOLPI, C. L. FINK, G. E. MARSH, E. A. RHODES, and G. S. STANFORD, "Fast-Neutron Hodoscope at TREAT: Methods for Quantitative Determination of Fuel Dispersal", Nucl. Tech. **56**, 141 (1982).
4. R. SIMMS et al, "TREAT Experimental Data Base Regarding Fuel Dispersals in LMFBR Loss-of-Flow Accidents", Proceedings of Reactor Safety Aspects of Fuel Behavior, p. 2-207, ANS/ENS Topical Meeting (August 2-6, 1981).

M6 TRANSIENT HODOGRAPHS

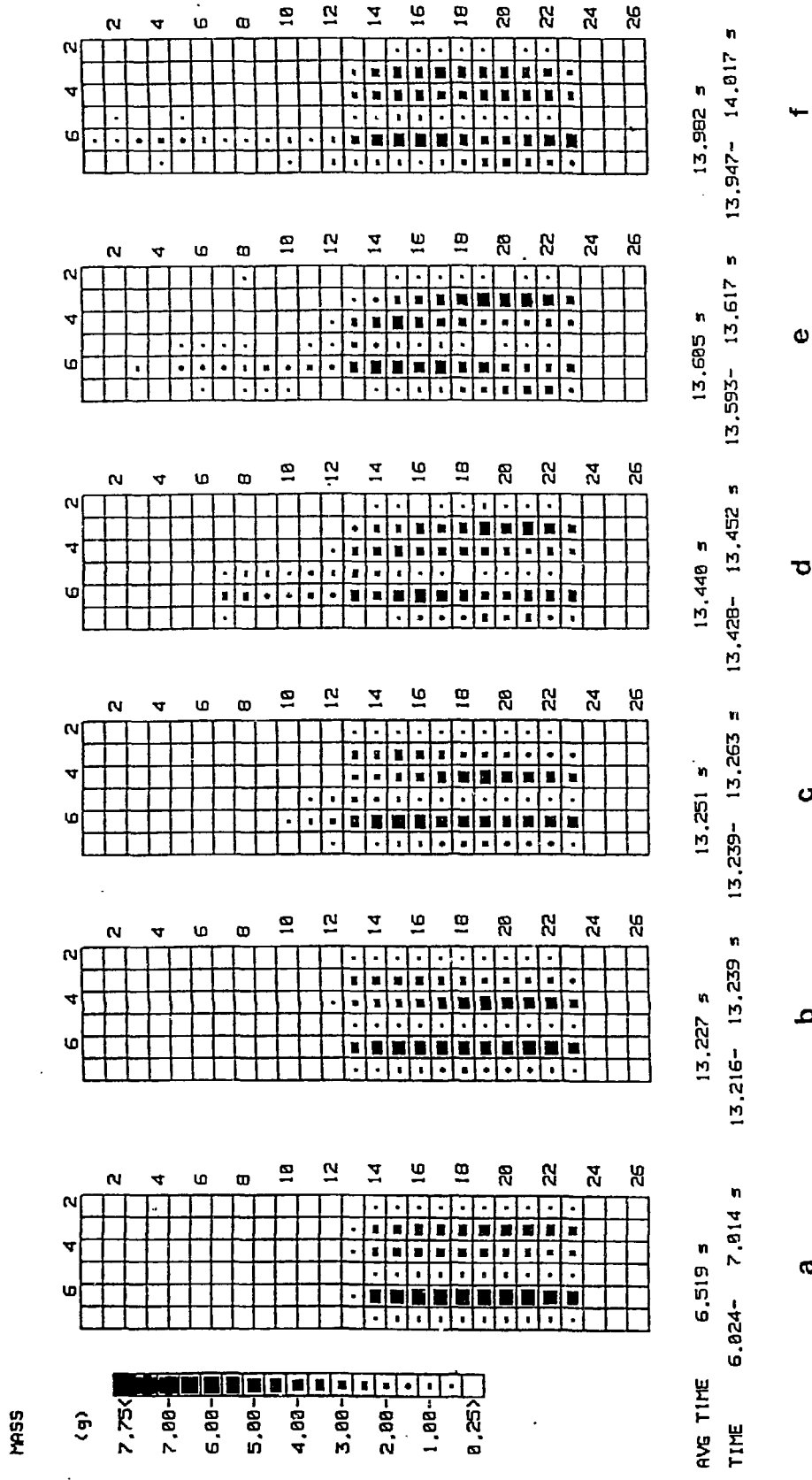


Fig. 9. Integral Hodographs at Selected Transient Times for Experiment M6

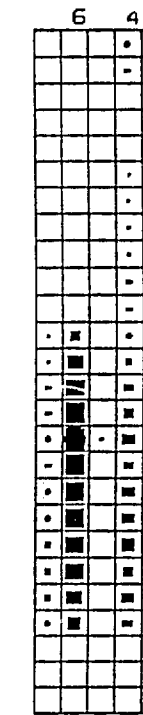
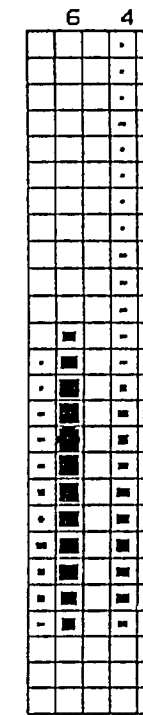
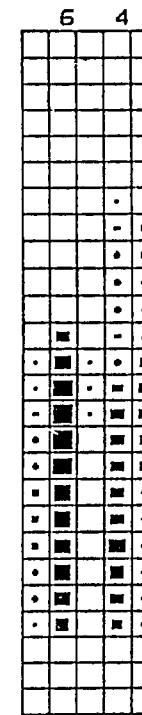
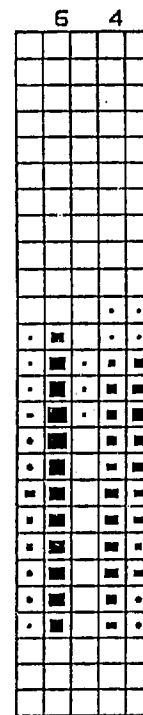
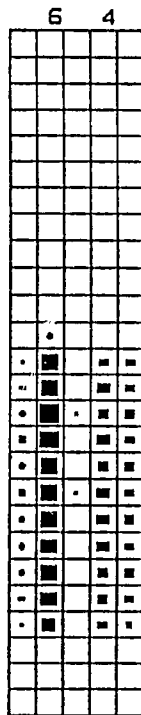
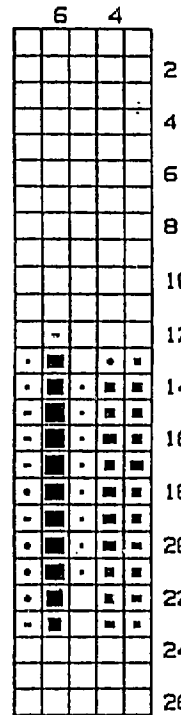
M7 TRANSIENT HODOGRAPHS

MASS

E W

(g)

7.75<
7.00-
6.00-
5.00-
4.00-
3.00-
2.00-
1.00-
0.25>



AVG TIME

9,503 s

17,102 s

17,408 s

17,710 s

17,844 s

18,349 s

20,518 s

TIME 8,982- 10,023 s 17,051- 17,153 17,357- 17,459 17,663- 17,757 17,757- 17,931 17,932- 18,765 19,916- 21,121

a

b

c

d

e

f

g

Fig. 10. ² Integral Hodographs at Selected Transient Times for Experiment M7

M5F1 WORTH

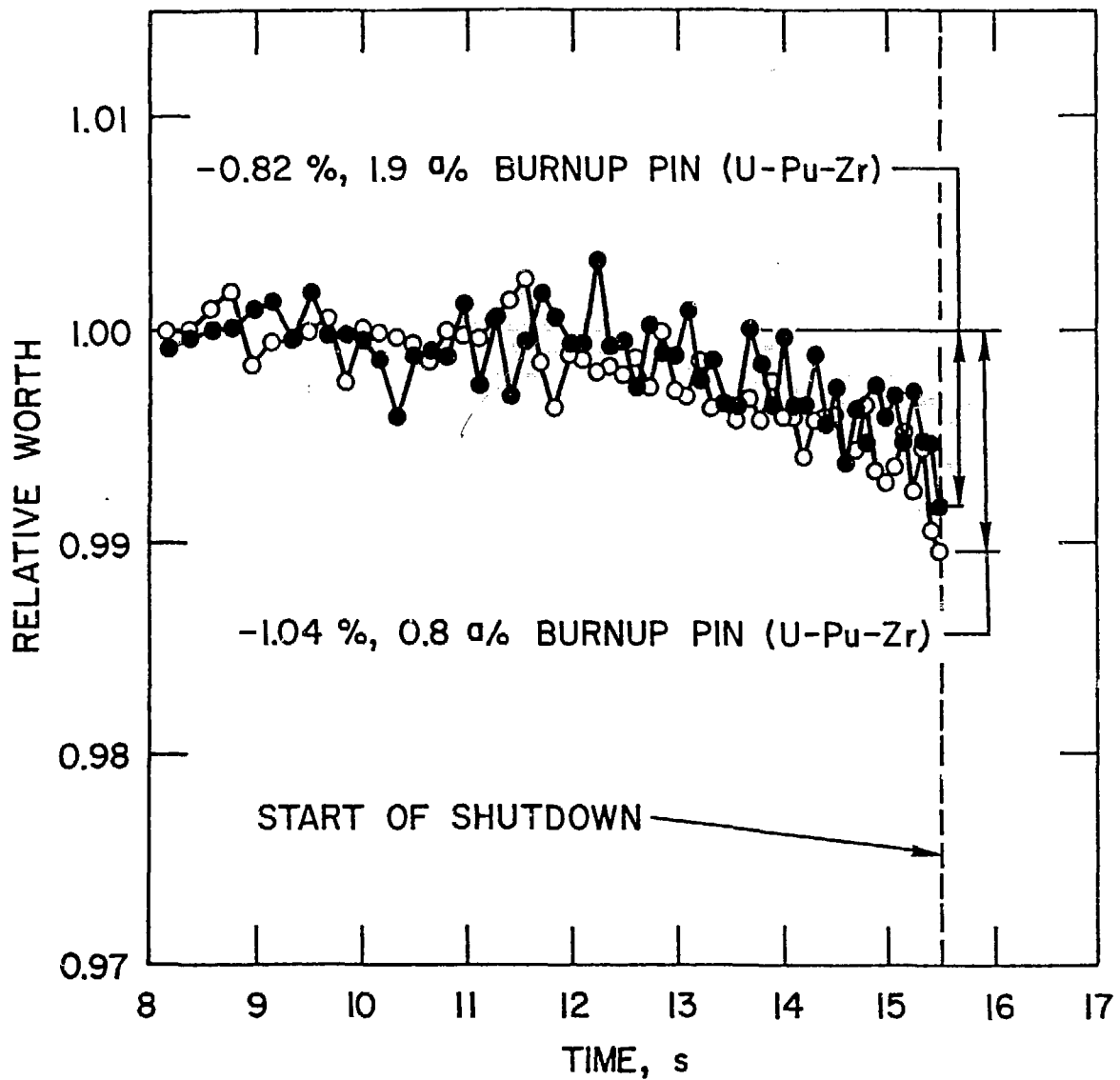


Fig. 14. Relative Worth vs. Elapsed Transient Time for Experiment M5F1

M5F2 WORTH

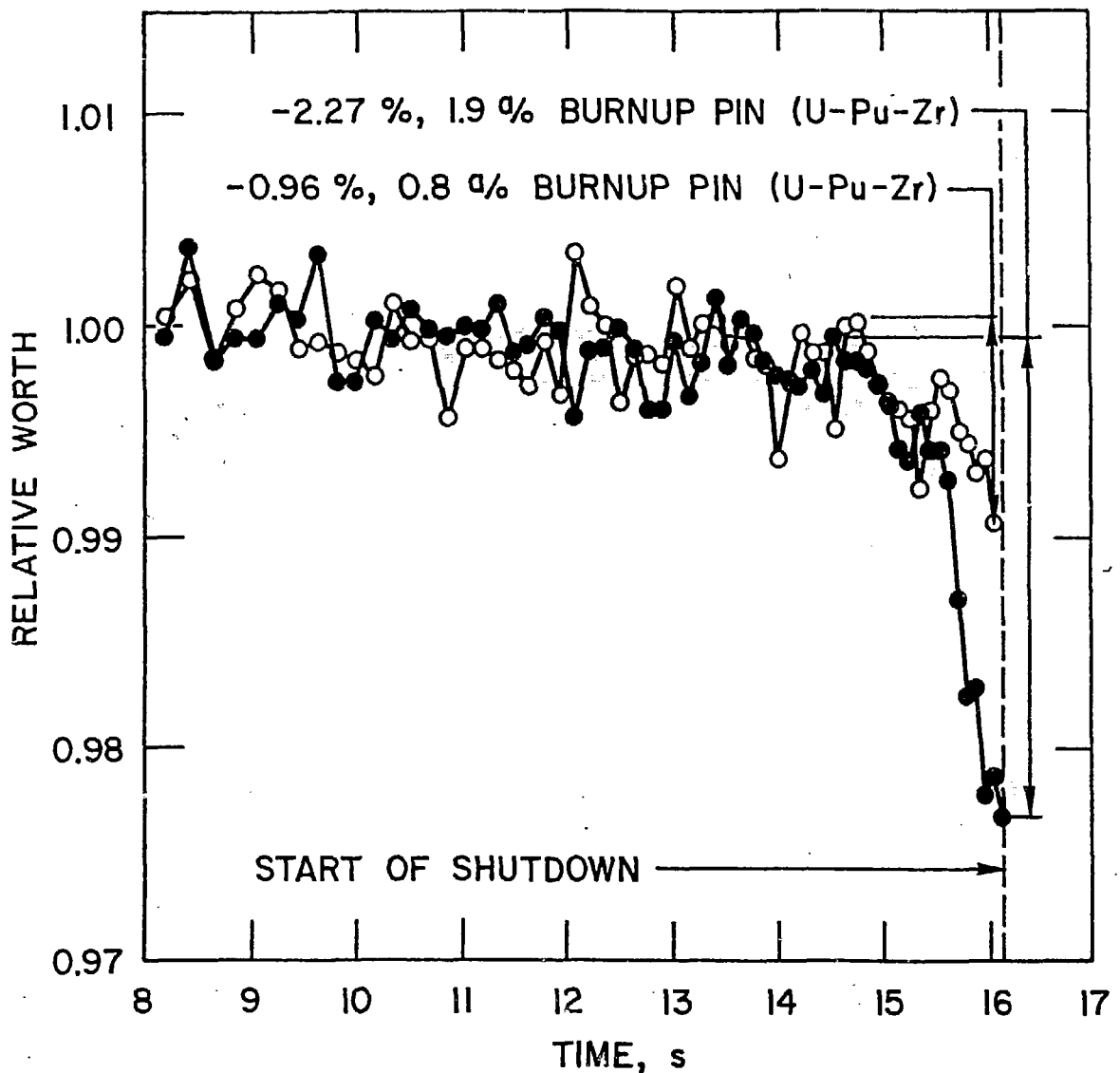


Fig. 15. ⁴ Relative Worth vs. Elapsed Transient Time for Experiment M5F2

M6 WORTH

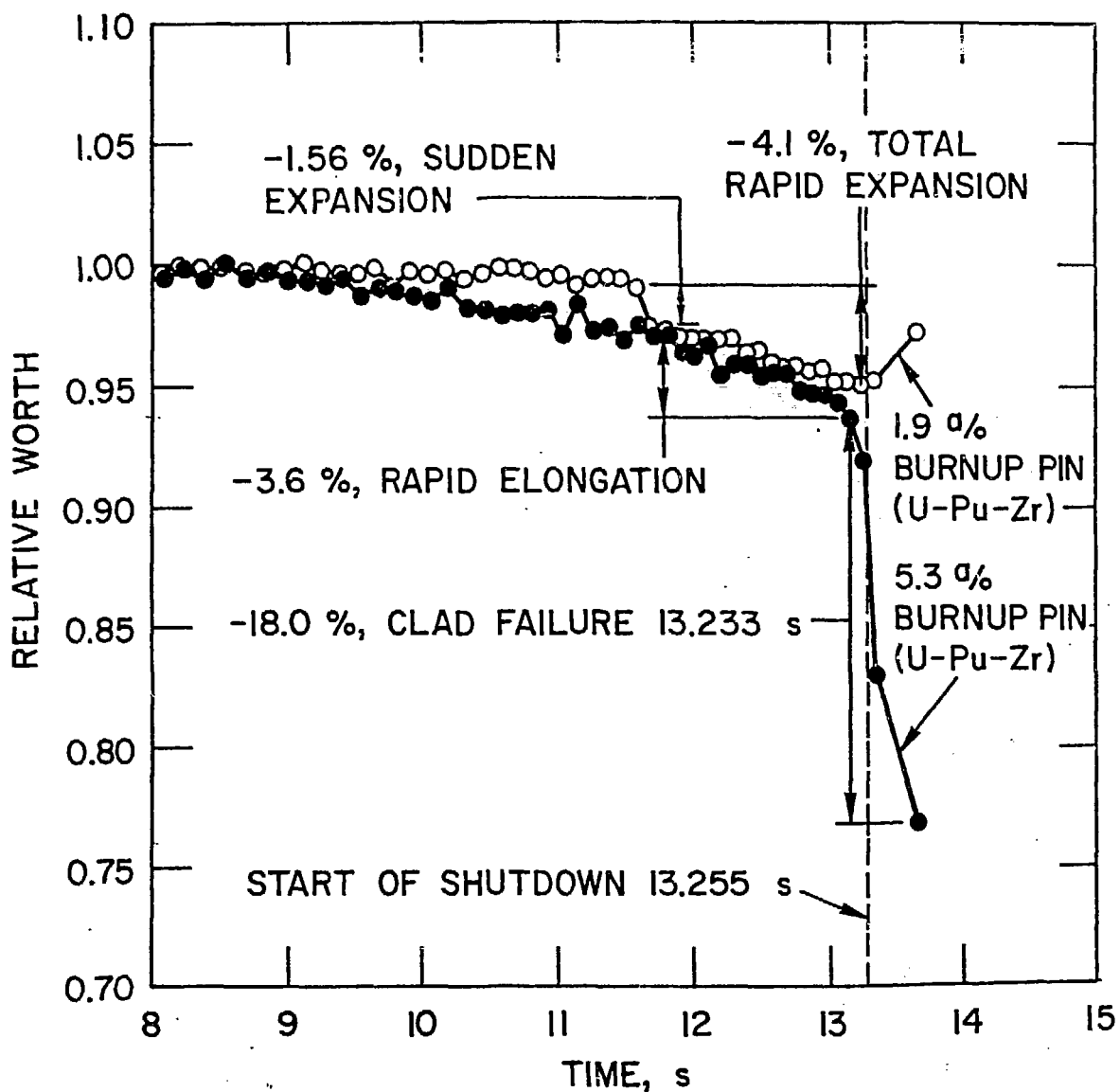


Fig. 16. Relative Worth vs. Elapsed Transient Time for Experiment M6

M7 WORTH

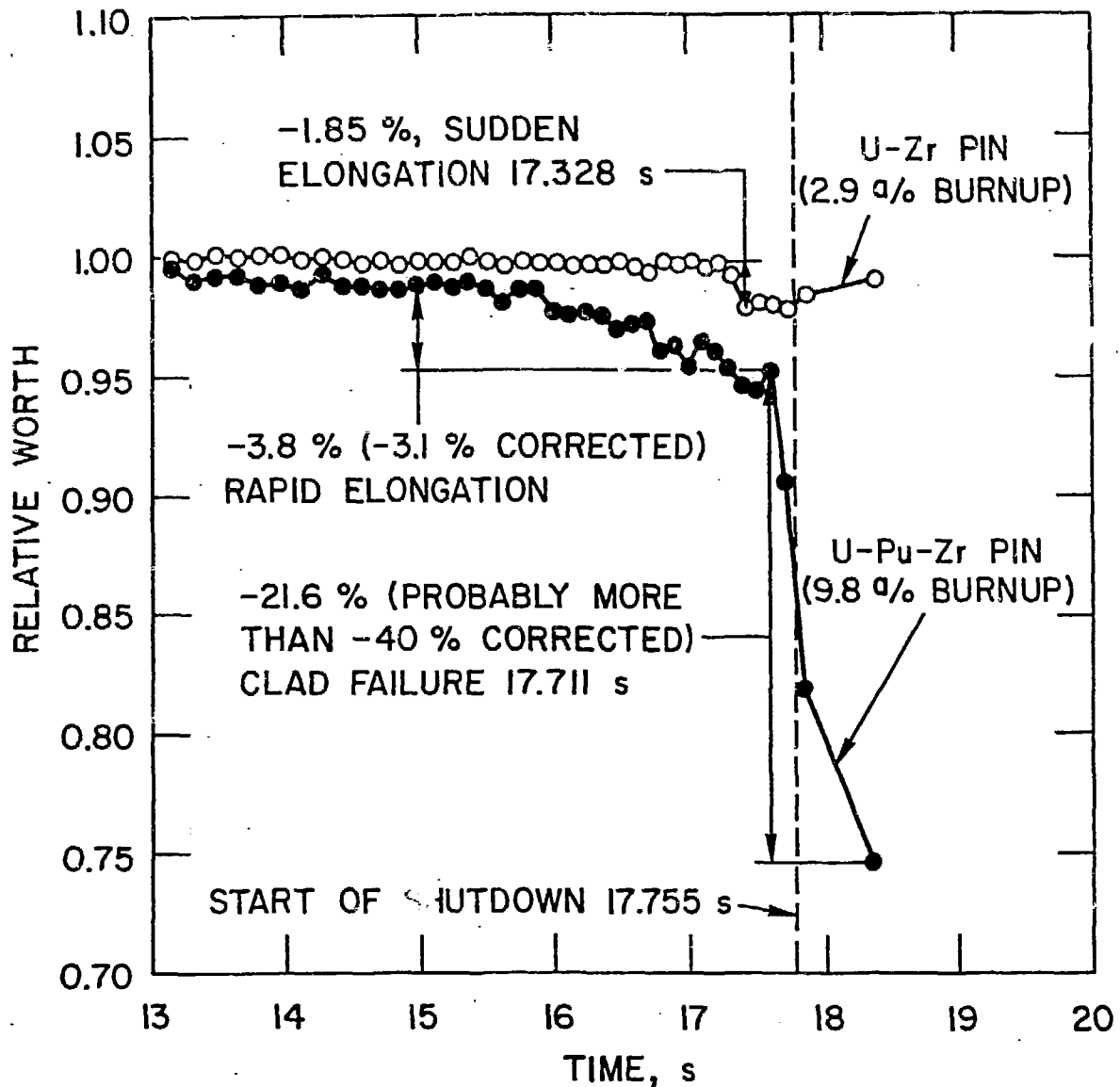


Fig. 17. Relative Worth vs. Elapsed Transient Time for Experiment M7